IEEE Photonics Journal
An IEEE Photonics Society Publication

Open Access

Microwave Photonic Bandpass Filter Based on Carrier-Suppressed Single Sideband Injected Distributed Feedback Laser

Volume 9, Number 3, June 2017

Huatao Zhu
Rong Wang
Peng Xiang
Tao Pu, ***Member, IEEE***
Jilin Zheng
Yuandong Li
Tao Fang
Long Huang
Yu Han
Xiangfei Chen, ***Senior Member, IEEE***

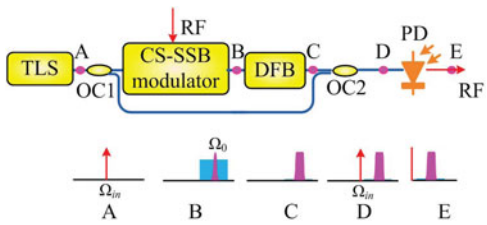

DOI: 10.1109/JPHOT.2017.2698072
1943-0655 © 2017 IEEE

IEEE photonics SOCIETY

IEEE

Microwave Photonic Bandpass Filter Based on Carrier-Suppressed Single Sideband Injected Distributed Feedback Laser

Huatao Zhu,[1] Rong Wang,[1] Peng Xiang,[1] Tao Pu,[1] *Member, IEEE*, Jilin Zheng,[1] Yuandong Li,[1] Tao Fang,[1] Long Huang,[2] Yu Han,[1] and Xiangfei Chen,[2] *Senior Member, IEEE*

[1]College of Communications Engineering, PLA University of Science and Technology, Nanjing 210007, China
[2]School of Engineering and Applied Sciences, Nanjing University, Nanjing 210093, China

DOI:10.1109/JPHOT.2017.2698072

Manuscript received March 8, 2017; revised April 18, 2017; accepted April 23, 2017. Date of publication April 28, 2017; date of current version May 8, 2017. This work was supported in part by the National Natural Science Foundation of China under Grant 61475193, Grant 61504170, Grant 61671306, and Grant 61174199 and in part by the Natural Science Foundation of Jiangsu Province under Grant BK20140069. Corresponding author: Jilin Zheng (e-mail: zhengjilinjs@126.com).

Abstract: A novel microwave photonic filter (MPF) based on carrier-suppressed single sideband (CS-SSB) injected distributed feedback (DFB) laser is proposed. The proposed MPF system exploits the frequency selective gain feature of optical injected DFB lasers, which can be tuned by adjusting the optical injection parameters or the working conditions of the laser. Therefore, the proposed MPF system can be tunable. The proposed system is verified by a proof-of-concept experiment, and the results show that the passband of the proposed MPF can be tuned by tuning the injection ratio and bias current of the slave laser, where the tuning range of 9–39 GHz is realized. At the same time, the out-of-band rejection of the proposed MPF can reach to 32 dB. Moreover, a dual-passband MPF response is also realized by the proposed system with a couple of master lasers, and the two passbands can be tuned independently from 10 to 39 GHz.

Index Terms: Microwave photonic filter, semiconductor lasers, optical injection.

1. Introduction

Microwave photonic filters (MPFs) have attracted a lot research interest in the past decades, which can find applications in radar, electronic warfare, radio astronomy, and future fifth-generation (5G) wireless communications [1]. Compared with traditional microwave filters, MPFs have shown superior advantages in terms of immunity to electromagnetic interference (EMI), wideband, large frequency tunability, and reconfigurability [2]–[5]. Various MPF schemes have been proposed in the literature. MPF is typically implemented by delay-line configuration with a finite-impulse response [6]–[8] or infinite-impulse response [9], [10], which belongs to incoherent MPF. However, the tunability of this kind of MPF, which is usually realized by tuning its optical delay-line module, is limited by its periodic frequency response. Different from the incoherent MPF, coherent MPF typically consists of a narrow linewidth light source, an optical modulator and one or two cascaded optical filter. The

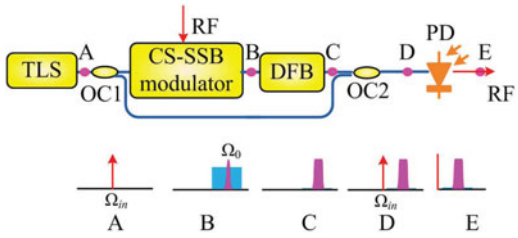

Fig. 1. Schematic diagram of the CS-SSB injection based MPF. TLS: tunable laser source; RF: radio frequency signal; CS-SSB: carrier-suppressed single sideband; DFB: distributed feedback laser; OC: optical coupler; PD: photodetector.

filter can be implemented in the optical domain, such as using tunable optical bandpass filter [11], phase-shift fiber Bragg grating [12], stimulated Brillouin scattering (SBS) effect in optical fiber [13], [14] or on chip [15], Lyot loop filter [16], and optical injected distributed feedback (DFB) laser [17], [18]. Among these schemes, the optical injected DFB laser based MPF shows superior performance in terms of compact structure, widely tunability and low loss. However, its out-of-band suppression ratio is limited by the four-wave mixing (FWM) dynamics [19] and the reconfiguration of bandwidth is limited [18].

In this paper, a bandpass MPF based on carrier-suppressed single sideband (CS-SSB) optical injected DFB laser is proposed. The injected sideband with suppressed optical carrier can get frequency dependant amplification, due to the frequency-selective gain spectrum of the slave laser, and compared with previous work [19], FWM effects are reduced through optical carrier suppression. Then after beating the optical carrier and the output signal from slave laser, the gain spectrum of the optical injected laser is translated to the MPF frequency response. Besides, the frequency response of the proposed MPF can be tuned and reconfigured by adjusting the gain spectrum of the slave laser through the changing of the laser and injection parameters. A proof-of-concept experiment is carried out. Gain spectrum of the slave laser is measured. Then the frequency response of the MPF is measured under different detuning frequencies, injection ratios and bias currents of the slave laser. Both single passband and dual-passband responses are achieved based on the proposed scheme. The results show the central frequency of the passband can be widely tuned and the bandwidth of passband is also reconfigurable. The out-of-band rejection of the MPF is also investigated. The rest of this paper is organized as follows. Section 2 describes the principle of the MPF based on CS-SSB optical injected DFB laser. A proof-of-concept experiment is presented in Section 3, which is followed by the discussions and the conclusion in Section 4.

2. Principle

Fig. 1 shows the schematic diagram of the proposed MPF based on CS-SSB injected DFB laser. The proposed MPF consists of a tunable laser source (TLS), two 50:50 optical couplers (OCs), a CS-SSB modulator, a DFB laser and a photodetector (PD). The TLS functions as the master laser, part of its output continuous wave (CW) light is directed to the CS-SSB modulator for CS-SSB modulation, and the other part bypasses the modulators and the DFB and combined with the output of the DFB at the OC2, as shown in Fig. 1. The CS-SSB modulator mainly consists of a dual-parallel Mach-Zehnder modulator (DPMZM) which is driven by a radio frequency (RF) signal and a 90° hybrid power splitter [20], [21]. For the CS-SSB modulation, the upper sideband is retainned while the optical carrier and lower sideband are suppressed. The CS-SSB modulated signal is then injected into the DFB laser, which functions as the slave laser. The gain provided by the slave laser depends on the slave laser parameters and the injection parameters. The output signal from the slave laser is with another part of optical carrier through OC2 as shown in Fig. 1. Then the combined signals are detected by a PD, where the optical carrier is beaten with the amplified sideband. The magnitude of the RF signal output from the PD corresponds with the amplified

sideband. Thus, the frequency response of the proposed MPF has the same shape as the gain spectrum of the slave laser. Since the gain spectrum exhibits bandpass response in the optical domain [22], the MPF will present bandpass frequency response.

As shown in Fig. 1, the optical carrier from the master laser is CW lightwave at A point and its electrical field can be expressed as

$$E_{in}(t) = A_{in} \exp[j\Omega_{in} t + j\phi_{in}] \tag{1}$$

where A_{in}, Ω_{in} and ϕ_{in} are the optical intensity, angular frequency, and phase of the optical carrier, respectively. After the CS-SSB modulator, the signal at B point can be written as

$$E_{in}(\omega) \approx j2\pi A_{in} J_1\left(\frac{\pi V_{RF}}{V_\pi}\right) \delta(\Omega - \Omega_{in} - \omega_{RF}) \tag{2}$$

where V_{RF} and ω_{RF} are the amplitude and angular frequency of the RF signal, respectively. V_π is the half-wave voltage of the PM and J_1 denotes the 1st-order Bessel function of the first kind. According to the coupled wave theory of DFB laser [23], the gain spectrum of the slave laser can be expressed as [22]

$$G(\Omega) = \left|\cosh(\gamma L) - \frac{\alpha - j\sigma}{\gamma} \sinh(\gamma L)\right|^{-2} \tag{3}$$

where γ is a complex propagation constant, L denotes the cavity length of the slave laser, α is the mode gain per unit length. σ denotes complex detuning angular frequency and can be described as

$$\sigma \approx n(\Omega - \Omega_0)/c \tag{4}$$

where n denotes refractive index, Ω_0 is the Bragg frequency and c is the light velocity. Thus, the signal output from the slave laser at C point in Fig. 1 can be written as

$$E_{out}(\Omega) \propto jG(\Omega) A_{in} J_1\left(\frac{\pi V_{RF}}{V_\pi}\right) \delta(\Omega - \Omega_{in} - \omega_{RF}). \tag{5}$$

After the OC, the signal at D point can be described as

$$E_{out}(\Omega) = A_{in}\delta(\Omega - \Omega_{in}) + jG(\Omega) A_{in} J_1\left(\frac{\pi V_{RF}}{V_\pi}\right) \delta(\Omega - \Omega_{in} - \omega_{RF}). \tag{6}$$

After square-law detection in the PD, the output RF signal at E point can be written as

$$\begin{aligned} I(\omega) &= \left\langle \frac{1}{2\pi} \int_0^{+\infty} E_{out}(\Omega) E_{out}^*(\Omega - \omega) d\Omega \right\rangle \\ &= \frac{A_{in}^2}{2\pi} \int_0^{+\infty} \left[jJ_1\left(\frac{\pi V_{RF}}{V_\pi}\right) G(\Omega)\delta(\Omega - \omega - \Omega_{in})\delta(\Omega - \Omega_{in} - \omega_{RF}) \right] d\Omega \\ &= \frac{A_{in}^2}{2\pi} jJ_1\left(\frac{\pi V_{RF}}{V_\pi}\right) G(\Omega_{in} + \omega)\delta(\omega - \omega_{RF}). \end{aligned} \tag{7}$$

The injected RF signal is $2\pi[\delta(\omega - \omega_{RF}) + \delta(\omega + \omega_{RF})]$; thus the frequency response is expressed as

$$H(\omega) = \frac{A_{in}^2}{2\pi} jJ_1\left(\frac{\pi V_{RF}}{V_\pi}\right) G(\Omega_{in}+, \omega). \tag{8}$$

As can be seen from (8), the frequency response of the proposed MPF is mapped from the gain spectrum of the slave laser. Since the gain spectrum has a single bandpass shape [22], the MPF has a single passband. By adjusting parameters of the slave laser, the gain spectrum can be reconfigured, consequently, the accordingly frequency response of the MPF can be reconfigured. In addition, by changing Ω_{in}, the central frequency of the MPF's passband can be widely tuned.

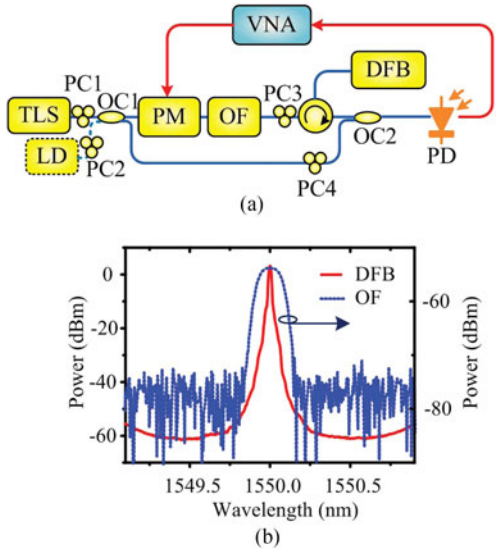

Fig. 2. (a) Experimental setup of the proposed MPF. (b) Transmission spectrum of the OF and the spectrum of the free running slave laser. TLS: tunable laser source; LD: laser diode; PC: polarization controller; OC: optical coupler; PM: phase modulator; OF: optical filter; DFB: distributed feedback laser; PD: photodetector; VNA: vector network analyzer.

By adding another optical carrier, which is written by $A_{in2}\exp(j\Omega_{in2}t + j\phi_{in2})$, to the PM with the same processing as the carrier in (1), the frequency response of the MPF can be easily achieved and described by

$$H(\omega) = \frac{A_{in}^2}{2\pi} jJ_1\left(\frac{\pi V_{RF}}{V_\pi}\right) G(\Omega_{in} + \omega) + \frac{A_{in2}^2}{2\pi} jJ_1\left(\frac{\pi V_{RF}}{V_\pi}\right) G(\Omega_{in2} + \omega). \tag{9}$$

Equation (9) shows the MPF has dual-passband when the Ω_{in} is different with Ω_{in2}. The central frequencies of the two passbands can be tuned independently by adjusting the value of Ω_{in} and Ω_{in2}, respectively. And multiple-passband MPF maybe realized by adding optical carriers with different central wavelengths.

3. Experimental Setup and Results

A proof-of-concept experiment is carried out to verify the proposed MPF and the experimental setup is shown in Fig. 2(a). A TLS, which acts as the master laser, is connected to polarization controller (PC1) to adjust the polarization state of the optical carrier. Another master laser with central wavelength of 1549.71 nm followed by PC2 is coupled with TLS through an 50:50 OC (OC1). The CS-SSB modulator is replaced by a PM and an OF due to the lack of RF hybrid coupler. The PM generates dual-sideband modulated signal and the OF filter out one sideband only to achieve CS-SSB modulated signal. The 3-dB bandwidth of the PM is 40 GHz. The central wavelength and 3-dB bandwidth of the OF are 1550.00 nm and 0.16 nm, respectively. A DFB laser with a central wavelength of 1550.00 nm and a threshold current of 9 mA is utilized as the slave laser. Fig. 2(b) shows the measured transmission spectrum of the OF and spectrum of the free running slave laser. The signal is launched into the slave laser through an optical circulator and PC3 is added to control the polarization state of the injected signal. Another 50:50 OC (OC2) is utilized to couple the signal from the slave laser with the signal from the master laser. The combined signals are detected by a PD with a bandwidth of 50 GHz and a responsivity of 0.65 A/W. A vector network analyzer (VNA, Anritsu MS4647A) is used to measure the frequency response of the proposed MPF. To measure the frequency response under different injection ratios, a variable optical attenuator (VOA), an OC and an optical power meter are added after the OF. The injection ratio is defined as the power

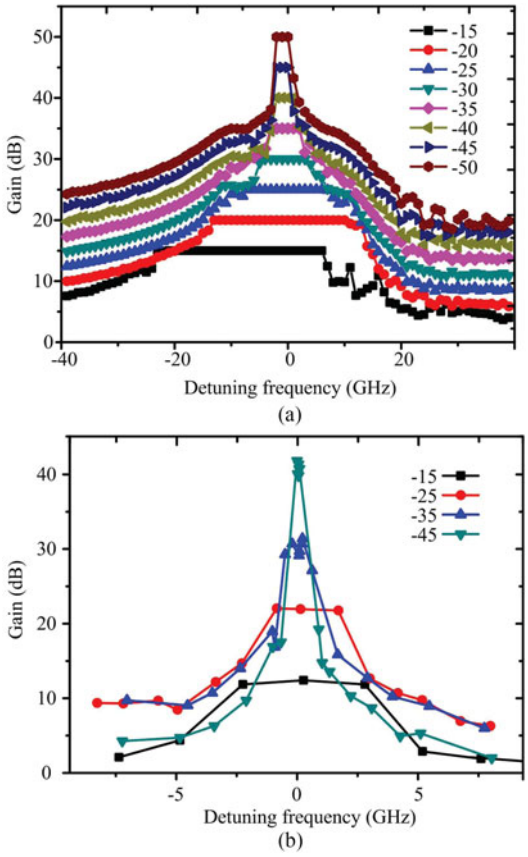

Fig. 3. (a) Simulated and (b) experimentally measured gain spectrum of the slave laser under different injection ratios.

ratio between the injected signal and free running slave laser, and detuning frequency is defined as $\Omega_{in} - \Omega_0$.

3.1. Gain Spectrum of Optical Injected DFB Laser

The frequency response can be described well by the coupled wave theory, however, when the slave laser is injection locked, the single mode rate equations describe the slave laser more precisely [24]. To analyse the gain spectrum of the slave laser in optical domain, a numerical simulation based on the single mode rate equation described in [25] and [26] is carried out. The gain spectrum in optical domain is achieved by $G(\Omega_{in}) = P_{out}\delta(\Omega - \Omega_{in})/P_{in}$, where P_{out} and P_{in} are the optical power of injected and output signal of the slave laser, respectively. The optical spectrum is measured by an optical spectral analyzer (OSA, Finisar Waveanalyzer 1500 s) with a maximum resolution of 150 MHz.

Fig. 3(a) shows the calculated gain spectrum and Fig. 3(b) presents the experimentally measured results under different injection ratios. As can be seen from Fig. 3(a), the bandwidth of the gain spectrum increases along with the injection ratio. This is because the gain grows to its maximum value in the locking range due to injection locking, and the bandwidth of the locking range is proportional to the square root of the injection ratio [27]. In addition, the central frequency of the gain spectrum slightly shifts to be lower as the improving of injection ratio. It is owing to the cavity resonance shift in DFB laser under optical injection [28]. The out-of-band suppression decreases as the enhancing of injection ratio. In the experimental measurement, the bias current of the

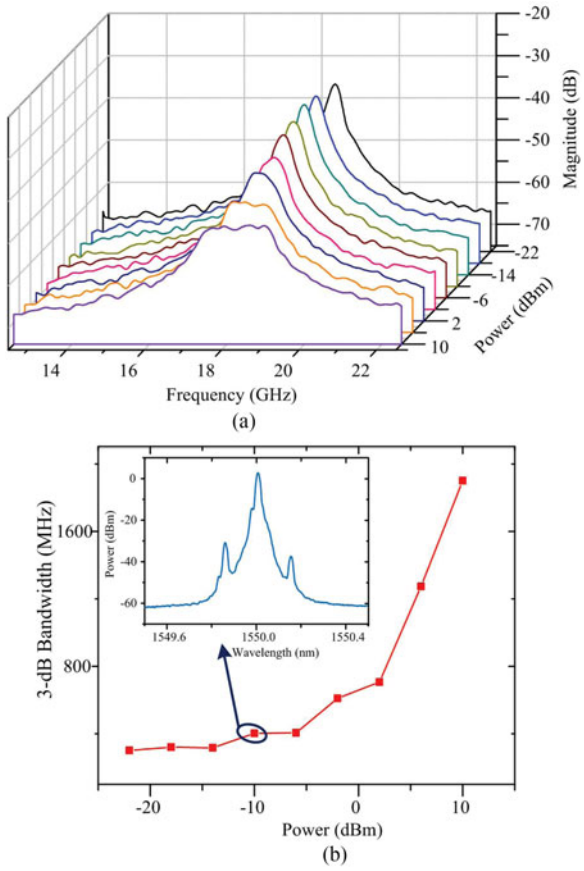

Fig. 4. (a) Measured frequency responses under different RF signal powers from VNA. (b) Corresponding bandwidth.

free-running slave laser is set as 35 mA. As the results shown, the experimental results agree well with the simulation results on the changing law.

3.2. Frequency Response of Single Passband MPF

Fig. 4(a) shows the frequency responses under different RF signal powers. Since the PM is under small signal modulation which means $V_{RF}/V_\pi \ll 1$, $J_1(\pi V_{RF}/V_\pi)$ approximates to $\pi V_{RF}/V_\pi$. Therefore the tuning of V_{RF} is equivalent to the adjustment of A_{in}^2 in (8). In other words, the tuning of RF signal power and injection ratio are equivalent when the bias current of the slave laser is fixed. The bias current of the slave laser is set as 35 mA and the detuning frequency is 18.5 GHz. As we can see, the MPF presents a response of single passband and the the out-of-band rejection increases as the decreasing of RF signal power. The frequency responses show the similar trend with the gain spectrum shown in Fig. 3. The corresponding 3-dB bandwidth is shown in Fig. 4(b). As the reduction of RF signal power, the 3-dB bandwidth is reduced. The maximum 3-dB bandwidth in Fig. 4(b) is 1.9 GHz and the minimum value is 301 MHz. When the RF signal power is 10 dBm, a flat top response is achieved resulting from the gain saturation effect. The flat region with a magnitude variation of 1.1 dB corresponds to the flat gain spectrum and locking range of slave laser. In practical application, the received RF signal power will be much less than 10 dBm, and the bandwidth of the MPF will be stable within a low variation when the RF signal power varies. In addition, the optical spectrum measured after the slave laser output is shown in Fig. 4(b). In Fig. 4(b) , the middle peak is the cavity mode of the slave laser, the lower peaks on its left and right sides are the residual optical

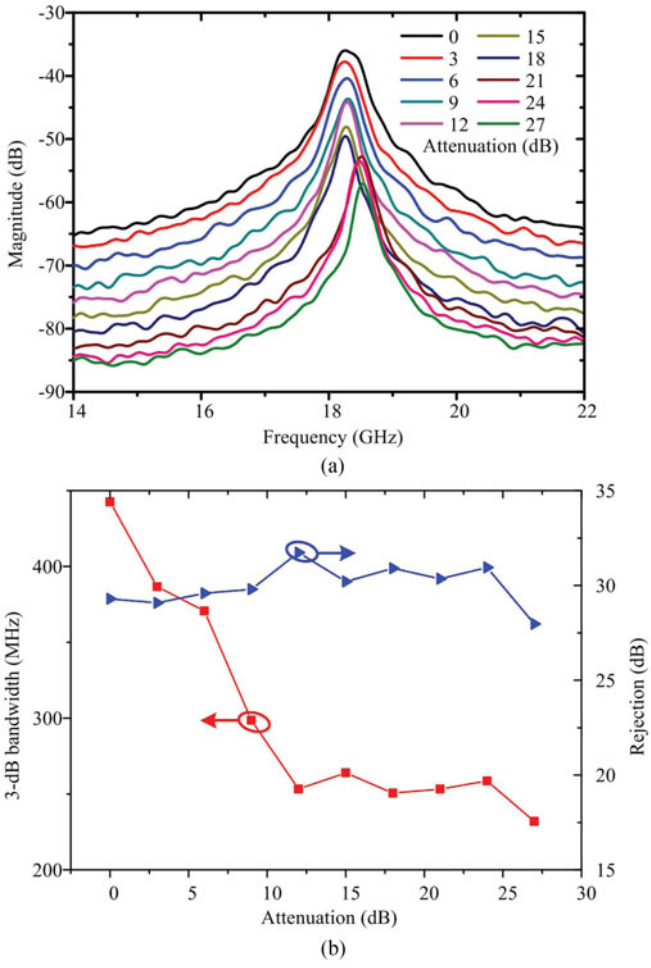

Fig. 5. (a) Measured frequency responses under different attenuations. (b) Corresponding bandwidth and out-of-band rejection.

carrier and the mixing signal due to FWM, respectively. Since the optical carrier is suppressed, the mixing signal is suppressed to be 40 dB less than the cavity mode. Furthermore, the affection of FWM effect on the MPF is reduced compared with other scheme [19].

The results in Fig. 4 are measured under a little big injection ratio. To investigate the frequency response under smaller injection ratio than above, a VOA is utilized to control different attenuations of the injected signal which means the adjustment of A_{in}^2 in (8). Fig. 5(a) shows the MPF response with different attenuations and Fig. 5(b) shows the MPF 3-dB bandwidth at different attenuations when its center frequency is set at 14 GHz. The RF signal power is set as -10 dBm, the bias current is 35 mA and the detuning frequency is 18.5 GHz. As the attenuation increases, the central frequency shifts to higher frequency due to the decrease of cavity resonance shift. The 3-dB bandwidth of the passband reduces along with the increasing of the attenuation, but the out-of-band rejection keeps around 30 dB. It is because the gain saturation effect disappears under weak injection, and the maximum gain is stable on this condition. The minimum 3-dB bandwidth in Fig. 5(b) is 232 MHz.

Next, the frequency responses under different bias currents are measured and the results are shown in Fig. 6. The RF signal power is set as -10 dBm, the attenuation is 0 dB and central wavelength of optical carrier is fixed. Since the changing of bias current results in the variation of central wavelength in free running slave laser, therefore, the detuning frequency changes and the central frequency of the passband shifts from 9 to 24 GHz. As the bias current increases, the

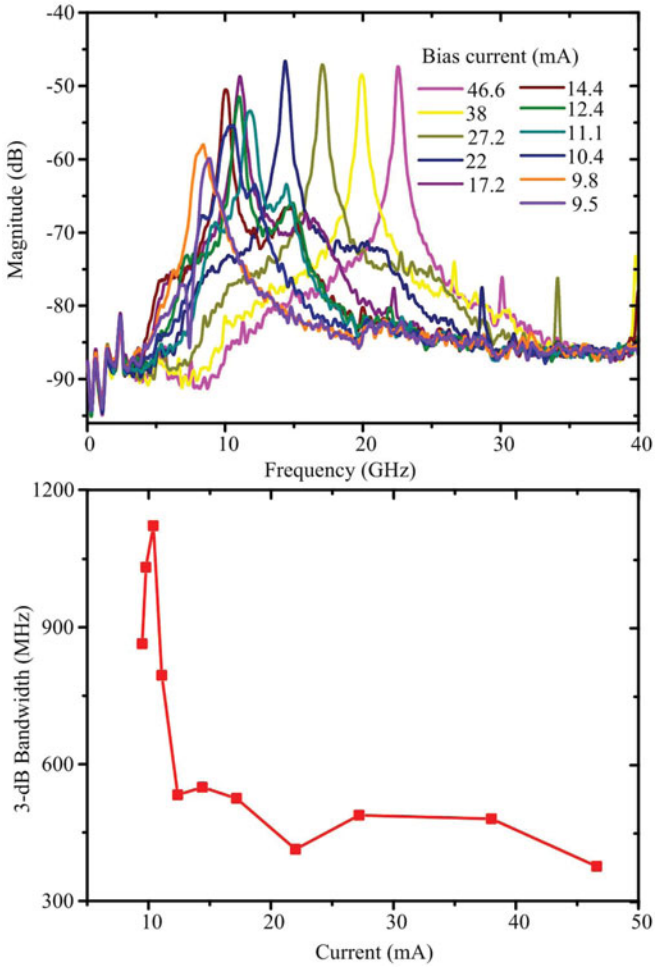

Fig. 6. (a) Measured frequency responses under different bias currents. (b) Corresponding bandwidth.

out-of-band rejection increases and the 3-dB bandwidth decreases. However, the bandwidth shows different value with other cases when the current is less than 10 mA because the injection ratio is large, and it is influenced by the residual optical carrier.

Then, under different detuning frequencies, the responses are measured as shown in Fig. 7. The attenuation is set as 0 dB, the bias current is 35 mA and RF signal power is set as −10 dBm. By tuning the central wavelength of the TLS, the detuning frequency is tuned from 39 GHz to −38 GHz, and the response shape keeps all the same when the optical carrier is suppressed. The out-of-band rejection is 32.3 dB when the detuning frequency is 14.3 GHz. Comparing the central frequency of passband under positive with negative detuning frequency, one can see that the two curves comply with each other. It shows that central frequency of passband is proportional to the absolute value of detuning frequency. The central frequency of passband can be continuously tuned from 9 to 39 GHz. When the detuning frequency ranges from −12 GHz to 8 GHz, the optical carrier is not suppressed and it results in the disordered responses. The lower end of center frequency of the proposed MPF is limited by experimental conditions. This issue may be solved by replacing the PM and OF by a DPMZM and a 90° hybrid power splitter to realize CS-SSB modulation [21]. The higher end of the center frequency of the proposed MPF is limited by the optical modulator. A higher central frequency of passband is possible to be achieved once the optical modulator with larger bandwidth is provided.

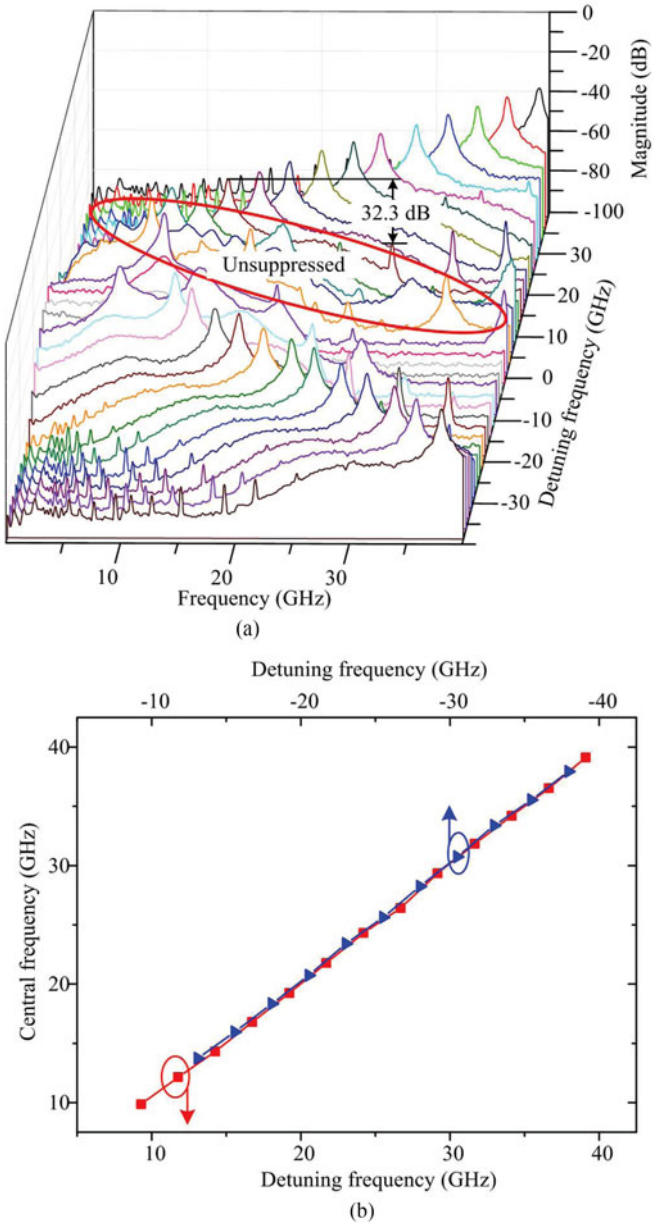

Fig. 7. (a) Measured frequency responses under different detuning frequencies. (b) Central frequency of passband.

3.3. Frequency Response of Dual-Passband MPF

Dual-passband MPF based on the proposed scheme is studied. The bias current is 35 mA, the attenuation is 0 dB and RF signal power is set as −10 dBm. Coupling two master lasers, the frequency response of the MPF is shown in Fig. 8(a). The wavelength of first master laser in this experiment is fixed, while the second is the TLS used in the upper subsections. As we can see, two passbands with central frequencies of 13.6 GHz and 32.1 GHz are achieved. The 3-dB bandwidths of the first and second passband are 366 MHz and 360 MHz, respectively, and the out-of-band rejections for the first and second passband are 23.1 dB and 24.7 dB, respectively. By adjusting the central wavelength of the TLS, the frequency responses are measured as shown in Fig. 8(b). The central frequency of the second passband is independently and continuously tuned from 10 GHz

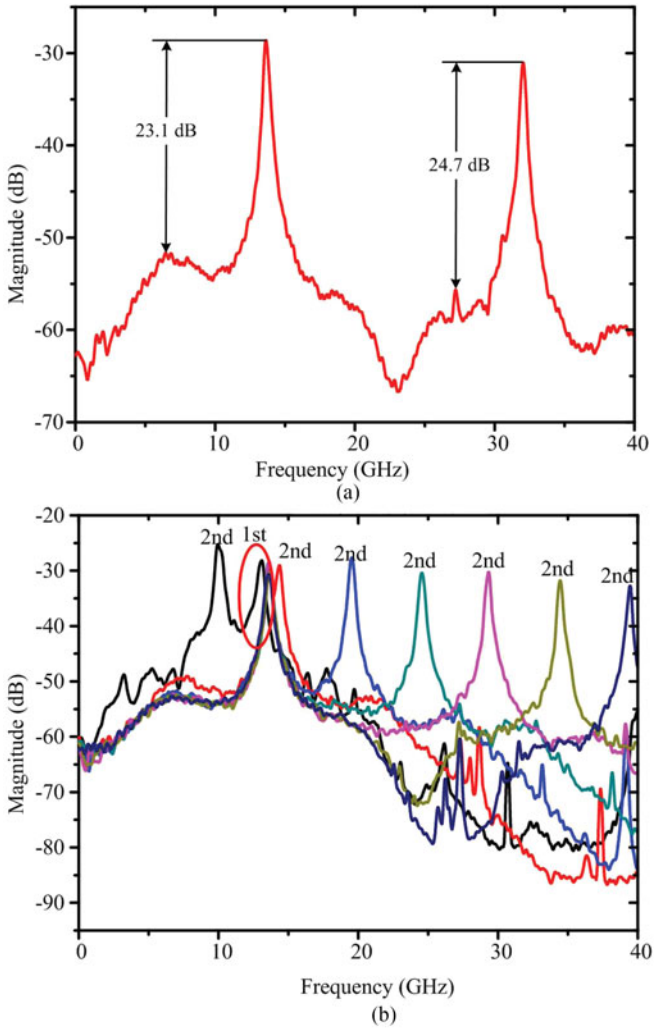

Fig. 8. (a) Measured response of the dual-passband MPF. (b) Responses under different detuning frequencies.

to 39 GHz, while the first passband keeps fixed. The first passband could also be tuned once the LD is replaced with another TLS.

4. Discussions and Conclusion

The first issue to be discussed is the influence of the nonlinear dynamics in the optical external injected slave laser on the proposed MPF. Since the power of the injected sideband is small and the locking bandwidth in the proposed system is less than 2 GHz, the nonlinear dynamics, such as chaos and period two will not appear in the slave laser. Period one dynamics will exist in the slave laser, but the undesired signal can be effectively suppressed by the MPF with a out-of-band rejection shown in Section 3. Second, for the 3-dB bandwidth of the proposed MPF, the minimum value shown in Section 3 is 232 MHz in Fig. 5(b). Apart from the adjustment of the parameters shown in this paper, as shown in (3), the bandwidth can be further reduced by utilizing a DFB laser with long cavity as the slave laser. Third, since no optical amplifier is used in the proposed MPF and the input power to the PD is less than -3dBm, the insertion loss is −30 dB. This loss will be greatly reduced by utilizing an optical amplifier and a PD with high input power. The loss can also

be reduced by increasing the output power of the TLS and the bias current of the DFB laser. In addition, the proposed MPF is good for integration due to the simple and compact system structure.

In conclusion, a novel bandpass MPF based on CS-SSB injected DFB laser is proposed. The frequency response of the proposed MPF utilizes the frequency selective gain of optical injected DFB lasers. By tuning the detuning frequency and injection ratio, the out-of-band injection and center frequency can be tuned, and the bandwidth can be reconfigured. The proposed MPF is demonstrated by a proof-of-concept experiment. The results show that the central frequency of single passband can be continuously tuned from 9 GHz to 39 GHz by tuning the wavelength of optical carrier, the minimum 3-dB bandwidth is 232 MHz by tuning injection ratio, and the out-of-band rejections can reach to 32 dB. In addition, dual-passband frequency response can also be achieved by the proposed MPF, which is useful for certain applications. The central frequency of the dual-passband can be tuned from 10 GHz to 39 GHz, the 3-dB bandwidths can reach to 360 MHz and the out-of-band rejections can reach to 24 dB.

References

[1] R. J. Cameron, C. M. Kudsia, and R. R. Mansour, *Microwave Filters for Communication Systems: Fundamentals, Design, and Applications*. Hoboken, NJ, USA: Wiley, 2007.

[2] J. Yao, "Photonics to the rescue: A fresh look at microwave photonic filters," *IEEE Microw. Mag.*, vol. 16, no. 8, pp. 46–60, Sep. 2015.

[3] J. Capmany, B. Ortega, and D. Pastor, "A tutorial on microwave photonic filters," *J. Lightw. Technol.*, vol. 24, no. 1, pp. 201–229, Jan. 2006.

[4] J. Capmany, J. Mora, I. Gasulla, J. Sancho, J. Lloret, and S. Sales, "Microwave photonic signal processing," *J. Lightw. Technol.*, vol. 31, no. 4, pp. 571–586, Feb. 2013.

[5] X. Yi and R. Minasian, "Recent advances in single bandpass microwave photonic filtering," in *Proc. OptoElectron. Commun. Conf. Australian Conf. Opt. Fibre Technol.*, 2014, pp. 1027–1029.

[6] J. Yao, "Microwave photonics," *J. Lightw. Technol.*, vol. 27, no. 3, pp. 314–335, Feb. 2009.

[7] V. R. Supradeepa *et al.*, "Comb-based radiofrequency photonic filters with rapid tunability and high selectivity," *Nature Photon.*, vol. 6, no. 3, pp. 186–194, 2012.

[8] L. Huang *et al.*, "Microwave photonic filter with multiple independently tunable passbands based on a broadband optical source," *Opt. Exp.*, vol. 23, no. 20, pp. 25 539–25 552, 2015.

[9] L. Zhou, X. Zhang, E. Xu, Y. Yu, X. Li, and D. Huang, "A novel tunable cascaded IIR microwave photonic filter," *Opt. Commun.*, vol. 283, no. 14, pp. 2794–2797, 2010.

[10] Y. Jin *et al.*, "Gigahertz single source IIR microwave photonic filter based on coherence managed multi-longitudinal-mode fiber laser," *Opt. Exp.*, vol. 23, no. 4, pp. 4277–4288, 2015.

[11] Y. Yu *et al.*, "Switchable microwave photonic filter between low-pass and high-pass responses," *IEEE Photon. J.*, vol. 8, no. 5, pp. 1–8, Oct. 2016.

[12] W. Li, M. Li, and J. Yao, "A narrow-passband and frequency-tunable microwave photonic filter based on phase-modulation to intensity-modulation conversion using a phase-shifted fiber bragg grating," *IEEE Trans. Microw. Theory Techn.*, vol. 60, no. 5, pp. 1287–1296, May 2012.

[13] W. Zhang and R. A. Minasian, "Widely tunable single-passband microwave photonic filter based on stimulated brillouin scattering," *IEEE Photon. Technol. Lett.*, vol. 23, no. 23, pp. 1775–1777, Dec. 2011.

[14] L. Yi *et al.*, "Polarization-independent rectangular microwave photonic filter based on stimulated brillouin scattering," *J. Lightw. Technol.*, vol. 34, no. 2, pp. 669–675, Jan. 2016.

[15] R. Pant, D. Marpaung, I. V. Kabakova, B. Morrison, C. G. Poulton, and B. J. Eggleton, "On-chip stimulated brillouin scattering for microwave signal processing and generation," *Laser Photon. Rev.*, vol. 8, no. 5, pp. 653–666, 2014.

[16] J. Ge and M. P. Fok, "Passband switchable microwave photonic multiband filter," *Sci. Rep.*, vol. 5, 2015, Art. no. 15882.

[17] J. Xiong *et al.*, "A novel approach to realizing a widely tunable single passband microwave photonic filter based on optical injection," *IEEE J. Sel. Topics Quantum Electron.*, vol. 21, no. 6, pp. 171–176, Nov./Dec. 2015.

[18] Y. Deng, M. Li, J. Tang, S. Sun, N. Huang, and N. Zhu, "Widely tunable single-passband microwave photonic filter based on DFB-SOA-assisted optical carrier recovery," *IEEE Photon. J.*, vol. 7, no. 5, pp. 1–8, Oct. 2015.

[19] T. Zhang, X. Chen, J. Xiong, J. Zheng, and T. Pu, "Wideband tunable single bandpass microwave photonic filter based on FWM dynamics of optical-injected DFB laser," *Electron. Lett.*, vol. 52, no. 1, pp. 57–59, 2016.

[20] Y. Ogiso, Y. Tsuchiya, S. Shinada, S. Nakajima, T. Kawanishi, and H. Nakajima, "High extinction-ratio integrated Mach-Zehnder modulator with active y-branch for optical ssb signal generation," *IEEE Photon. Technol. Lett.*, vol. 22, no. 12, pp. 941–943, Jun. 2010.

[21] C. H. Wang, C. W. Chow, C. H. Yeh, C. L. Wu, S. Chi, and L. Chinlon, "Rayleigh noise mitigation using single-sideband modulation generated by a dual-parallel MZM for carrier distributed PON," *IEEE Photon. Technol. Lett.*, vol. 22, no. 11, pp. 820–822, Jun. 2010.

[22] K. Magari, H. Kawaguchi, K. Oe, and M. Fukuda, "Optical narrow-band filters using optical amplification with distributed feedback," *IEEE J. Quantum Electron.*, vol. 24, no. 11, pp. 2178–2190, Nov. 1988.

[23] H. Kogelnik and C. V. Shank, "Coupled-wave theory of distributed feedback lasers," *J. Appl. Phys.*, vol. 43, no. 5, pp. 2327–2335, 1972.

[24] R. Lang, "Injection locking properties of a semiconductor laser," *IEEE J. Quantum Electron.*, vol. QE-18, no. 6, pp. 976–983, Jun. 1982.
[25] J. Dellunde, M. C. Torrent, J. M. Sancho, and M. S. Miguel, "Frequency dynamics of gain-switched injection-locked semiconductor lasers," *IEEE J. Quantum Electron.*, vol. 33, no. 9, pp. 1537–1542, Sep. 1997.
[26] H. Zhu, R. Wang, T. Pu, P. Xiang, J. Zheng, and T. Fang, "A novel approach for generating flat optical frequency comb based on externally injected gain-switching distributed feedback semiconductor laser," *Laser Phys. Lett.*, vol. 14, no. 2, 2017, Art. no. 026201.
[27] C. J. Buczek, R. J. Freiberg, and M. L. Skolnick, "Laser injection locking," *Proc. IEEE*, vol. 61, no. 10, pp. 1411–1431, Oct. 1973.
[28] A. Murakami, K. Kawashima, and K. Atsuki, "Cavity resonance shift and bandwidth enhancement in semiconductor lasers with strong light injection," *IEEE J. Quantum Electron.*, vol. 39, no. 10, pp. 1196–1204, Oct. 2003.